JOURNAL OF SPACECRAFT AND ROCKETS
Vol. 29, No. 1, January-February 1992

Long Duration Exposure Facility Surface Temperatures

P. C. Hughes* and R. C. Tennyson†
University of Toronto, Downsview, Ontario, M3H 5T6 Canada

Temperatures on the surface of the Long Duration Exposure Facility (LDEF) depend on a number of factors. The LDEF is sometimes in sunlight, sometimes in eclipse; even when the LDEF is in sunlight, a particular surface area (e.g., a test patch) may not be able to see the Sun; and, finally, even if it can see the Sun, the angle of incidence of the Sun's radiation on the test patch is important. The heat input to the test patch from the rest of the LDEF vehicle depends on the average vehicle temperature, which in turn depends on its eclipse history. This paper examines all of these factors and uses a multiple-time-scale description (corresponding to orbital, precessional, and annual time scales) to build an understanding of the chief features observed in the flight data. Geometrical, orbital, and thermal models are developed. Numerical calculations based on these models are shown to be in general agreement with the characteristics of flight data. Thus, all of the salient features of the in-orbit temperature data can be explained in terms of the physical phenomena described.

Nomenclature

$\hat{a}_1,\hat{a}_2,\hat{a}_3$ = dextral orthonormal triad of unit vectors associated with the reference frame $\mathcal{F}_a$; see Fig. 3
C_{ba} = rotation matrix that transforms vector components in $\mathcal{F}_a$ to vector components in $\mathcal{F}_b$
C_{eb} = rotation matrix that transforms vector components in $\mathcal{F}_b$ to vector components in $\mathcal{F}_e$
C_{pe} = rotation matrix that transforms vector components in $\mathcal{F}_e$ to vector components in $\mathcal{F}_p$
$\hat{e}_1,\hat{e}_2,\hat{e}_3$ = dextral orthonormal triad of unit vectors associated with the reference frame $\mathcal{F}_e$; $\hat{e}_3$ is aligned with Earth's north pole, and $\hat{e}_1$ and $\hat{e}_2$ lie in Earth's equatorial plane
$\mathcal{F}_a$ = inertial reference frame whose center is at the Sun's center; see Fig. 3
$\mathcal{F}_b$ = reference frame parallel to $\mathcal{F}_a$ whose center is at Earth's center
$\mathcal{F}_e$ = reference frame centered at Earth's center and aligned with Earth's north pole and equator; note, however, that $\mathcal{F}_e$ does not have Earth's daily rotation
$\mathcal{F}_p$ = reference frame centered on LDEF when at perigee and aligned with LDEF's orbit around Earth; see Fig. 4
$\mathcal{F}_o$ = "orbiting" reference frame centered on LDEF and aligned with LDEF's orbit around Earth; see Fig. 4
h = LDEF altitude above Earth
i = inclination of LDEF's orbit with respect to $\mathcal{F}_e$
i_e = inclination of Earth's orbit with respect to the ecliptic plane
J_2 = Earth's oblateness factor
$\hat{o}$ = unit (outward) vector normal to the test patch on LDEF's surface; see Fig. 5
$\hat{o}_1,\hat{o}_2,\hat{o}_3$ = dextral orthonormal triad of unit vectors associated with the reference frame $\mathcal{F}_o$; $\hat{o}_3$ is vertically up toward LDEF from Earth's center, $\hat{o}_1$ is in the "forward" direction, and $\hat{o}_2$ is aligned with LDEF's orbit normal; see Fig. 4
P = LDEF's orbital period
$\hat{p}_1,\hat{p}_2,\hat{p}_3$ = dextral orthonormal triad of unit vectors associated with the reference frame $\mathcal{F}_p$; $\hat{p}_3$ is aligned with LDEF's orbit normal, and $\hat{p}_1$ and $\hat{p}_2$ lie in LDEF's orbital plane, with $\hat{p}_2$ pointing from Earth's center to LDEF when at perigee; see Fig. 4
r_e = Earth's equatorial radius
$\hat{s}$ = unit vector from the Sun to LDEF; see Fig. 3
T = temperature of test patch
T_v = average temperature of LDEF vehicle
t = time
η = true anomaly of LDEF in its orbit about Earth; see Fig. 4
η_e = true anomaly of the Earth in its orbit about the Sun; see Fig. 3
κ = heat input constant for the LDEF test patch; see Appendix
κ_v = heat input constant for the LDEF vehicle; see Appendix
λ = angle between $\hat{o}$ and $\hat{o}_2$ specifying the location of the test patch on the LDEF surface; see Fig. 5
μ_e = Earth's gravitational constant, 3.986×10^{14} m^3/s^2
τ = characteristic time lag for test patch
τ_v = characteristic time lag for the LDEF vehicle
φ = self-shadowing factor; see Eq. (16)
φ_v = Earth-shadowing factor; unity when $\hat{s}\cdot\hat{o}_3\leq0$; zero when $\hat{s}\cdot\hat{o}_3>0$
Ω = right ascension (argument of the ascending node) of LDEF's orbit with respect to $\mathcal{F}_e$
Ω_e = right ascension (argument of the ascending node) of the Earth's orbit with respect to the ecliptic plane
ω = argument of perigee of LDEF's orbit

Introduction

ONE of the purposes of the Long Duration Exposure Facility (LDEF) was to evaluate experimentally the effects of the low-Earth-orbit space environment on a variety of material specimens.[1,2] As part of these experiments, temperature data were collected to evaluate the test environment, and it is therefore helpful to understand the nature of these temperature data.

Two examples of such temperature data are shown in Figs. 1 and 2, over a period of about 1 yr. Note, however, that the circular dots are the data. The lines joining the dots have simply been drawn to join the dots. Thus, the solid lines do not

Received Nov. 15, 1990; revision received Oct. 10, 1991; accepted for publication Oct. 11, 1991.

*Professor, Institute for Aerospace Studies, 4925 Dufferin St. Associate Fellow AIAA.

†Director, Institute for Aerospace Studies, 4925 Dufferin St. Associate Fellow AIAA.

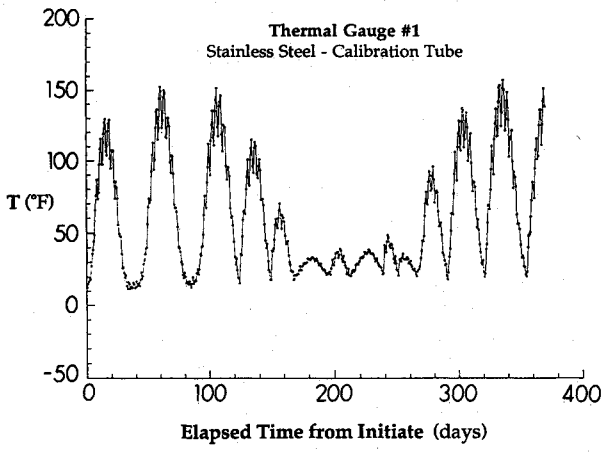

Fig. 1 LDEF temperature data for thermal gauge #1.

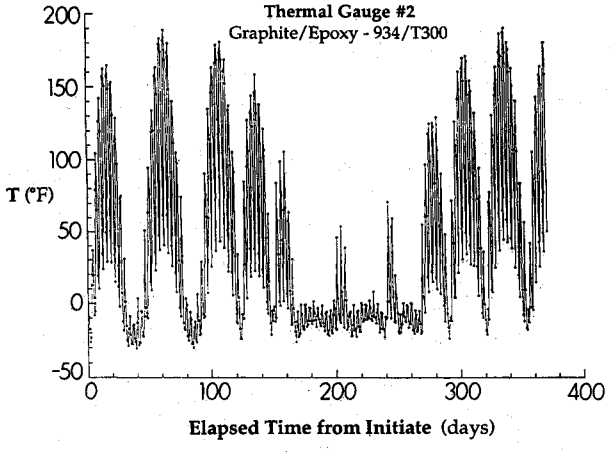

Fig. 2 LDEF temperature data for thermal gauge #2.

represent data. As we shall see presently, the solid lines do not follow—even approximately—actual (instantaneous) temperature histories, except in a time-averaged (slow-time-scale) sense.

This paper, which is a condensation and extension of Ref. 3, addresses the question of how to explicate the qualitative characteristics of these temperature data in simple physical terms. Relatively simple math models will be derived to gain physical understanding. The discussion is intended to be semiquantitative and physically motivated. Elaborate systems of partial differential equations or complex software packages for orbit dynamics or thermal analysis are avoided to promote physical transparency.

The qualitative features of these data can evidently be described in terms of three time scales: fast-time-scale changes (relatively rapid ~2-day oscillations), slow-time-scale changes (relatively slow ~45-day oscillations), and very-slow-time-scale changes (the even slower ~300-day oscillations). The primary purpose of this paper is to demonstrate the physical origin of these three superposed oscillations.

System Geometry

In this section we consider the purely geometrical problem of the angle of incidence of solar rays on a planar patch of material on the outside of the LDEF. The geometry will be defined using seven angles, some of which are constant, some of which are time varying.

Heliocentric Reference Frame

A series of needed reference frames is now introduced, proceeding from the Sun, in a sequence of stages, to the patch on the LDEF. The first frame, denoted $\mathcal{F}_a$, is shown in Fig. 3. The origin O_a is located at the Sun's center, and the frame is inertial (to the extent that the Sun's center is not accelerating—an excellent assumption for present purposes). The unit vectors associated with $\mathcal{F}_a$ are denoted by $\hat{a}_1$, $\hat{a}_2$, and $\hat{a}_3$. The unit solar vector, a vector from the Sun aimed at the LDEF satellite—aimed, to all intents and purposes, at the center of Earth—will be denoted by $\hat{s}$. It is evident from Fig. 3 that

$$\hat{s} \triangleq \hat{a}_1 \cos \eta_e + \hat{a}_2 \sin \eta_e \tag{1}$$

Geocentric Reference Frame

Still using Fig. 3, we have the second reference frame $\mathcal{F}_b$. The origin of $\mathcal{F}_b$ is displaced from the origin of $\mathcal{F}_a$ by the distance between Earth's and the Sun's centers. No new angles are thus introduced, however. In fact, the rotation matrix between $\mathcal{F}_b$ and $\mathcal{F}_a$ is just the unit matrix: $C_{ba} = 1$. Note that, although O_b is at Earth's center, the frame $\mathcal{F}_b$ is not fixed in Earth, nor is it even an equatorial frame. The rotation of Earth on its axis is, for present purposes, irrelevant. A geographic frame for Earth is, however, very important and will now be introduced.

Equatorial Reference Frame

The equatorial frame $\mathcal{F}_e$ has the following properties: O_e is located at Earth's center, and $\hat{e}_3$ coincides with Earth's north pole. It follows that the $\hat{e}_1$-$\hat{e}_2$ plane is Earth's equatorial plane. By introducing i_e, the inclination of Earth's polar axis to the ecliptic plane about an azimuthal direction given by Ω_e, one arrives at the standard result[4] that

$$C_{eb} = C_1(i_e)C_3(\Omega_e)$$

$$= \begin{bmatrix} \cos \Omega_e & \sin \Omega_e & 0 \\ -\cos i_e \sin \Omega_e & \cos i_e \cos \Omega_e & \sin i_e \\ \sin i_e \sin \Omega_e & -\sin i_e \cos \Omega_e & \cos i_e \end{bmatrix} \tag{2}$$

However, note that, although O_e is at Earth's center, and although $\hat{e}_3$ coincides with Earth's north pole, the frame $\mathcal{F}_e$ is not fixed in a rotating Earth. (As stated previously, Earth's rotation about its axis is irrelevant here.)

LDEF Orbit Reference Frame

Thus far, we have located Earth's poles and equatorial plane with respect to the ecliptic plane. No particular orbit has been specified. We now define this orbital plane with respect to $\mathcal{F}_e$ by its normal vector, using two angles i and Ω. The parameter (orbital element) i is the orbital inclination, and Ω is the argument of the ascending node.

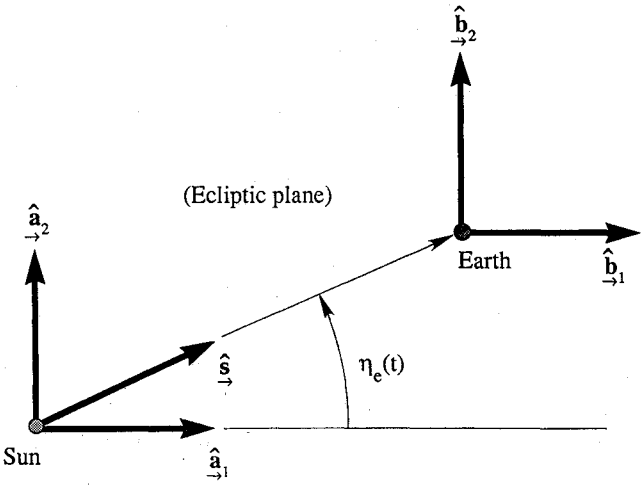

Fig. 3 The Sun-centered reference frame $\mathcal{F}_a$ and the (parallel) Earth-centered reference frame $\mathcal{F}_b$.

The orbit of the LDEF is then defined by the frame $\mathcal{F}_n$; specifically, the unit vectors $\hat{n}_1$ and $\hat{n}_2$ define the orbital plane. Thus, in a manner exactly paralleling Eq. (2),

$$C_{ne} = C_1(i)C_3(\Omega) = \begin{bmatrix} \cos\Omega & \sin\Omega & 0 \\ -\cos i \sin\Omega & \cos i \cos\Omega & \sin i \\ \sin i \sin\Omega & -\sin i \cos\Omega & \cos i \end{bmatrix} \tag{3}$$

And, of course, $C_{en} = C_{ne}^T$. In order for the orbit to have a unique set of orbital elements, these angles will be limited to the following ranges: $0 \le i \le \pi$, $0 \le \Omega \le 2\pi$.

Finally, following standard practice, we define the perigee frame $\mathcal{F}_p$ and let the perigee be located by a direction at angle ω to $\hat{n}_1$ within the orbital plane. Clearly ω gives the orientation of the orbit within the orbital plane. In fact,

$$C_{pn} \triangleq C_3(\omega) = \begin{bmatrix} \cos\omega & \sin\omega & 0 \\ -\sin\omega & \cos\omega & 0 \\ 0 & 0 & 1 \end{bmatrix} \tag{4}$$

However, we shall herein assume that the LDEF is always in an essentially circular orbit. Thus, the orbital eccentricity $e = 0$, and ω is undefined. Therefore, without any essential loss in generality, $C_{pn} = C_{np} = \mathbf{1}$, and

$$C_{pe} = C_{pn}C_{ne} = C_{ne} \tag{5}$$

$$C_{ep} = C_{pe}^T = C_{ne}^T \tag{6}$$

with C_{ne} given by Eq. (3).

Orbiting Reference Frame

Next we consider the position of the LDEF in its orbit. Consider Fig. 4, from which it may be deduced that the reference frame $\mathcal{F}_o$, which is fixed to the nominal spacecraft orientation in orbit, can be found from $\mathcal{F}_p$ as follows:

$$C_{op} = C_2\left(\frac{\pi}{2}+\eta\right)C_1\left(\frac{\pi}{2}\right) = \begin{bmatrix} -\sin\eta & \cos\eta & 0 \\ 0 & 0 & 1 \\ \cos\eta & \sin\eta & 0 \end{bmatrix} \tag{7}$$

The orbital anomaly $\eta(t)$ is the most rapidly changing variable.

Test Patch Unit Normal

Having established a nominal frame associated with the LDEF vehicle in orbit, we now consider the orientation of the test patch on the vehicle. However, it should be carefully noted

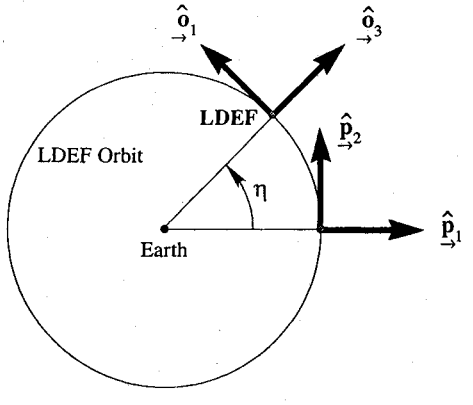

Fig. 4 The reference frame associated with LDEF in orbit, the orbiting frame $\mathcal{F}_o$.

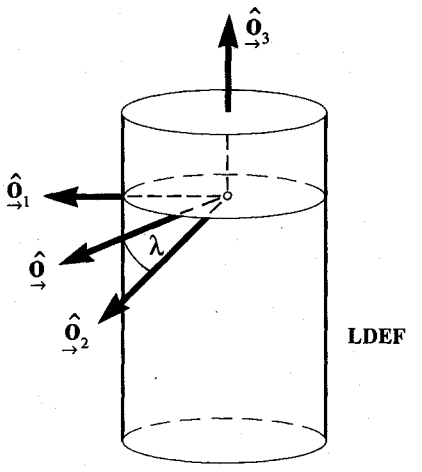

Fig. 5 The unit normal vector $\hat{o}$ outward from the test patch.

that at this point we are assuming no attitude librations of the vehicle with respect to the nominal frame $\mathcal{F}_o$. Equivalently, if there are such librations, they will be assumed to be negligible. Or, again equivalently, if there are such librations, and even if they are not instantaneously negligible, they will be assumed not to be large and to average out over a time period smaller than the fast-time-scale changes mentioned in the Introduction. That is, roll, pitch, and yaw will be assumed to be either identically zero, or negligible, or to be small and so rapid as to have no effect on the phenomena being studied. (Otherwise, an additional, body-fixed reference frame involving the three angles of roll, pitch, and yaw should be introduced[4] at this point.)

As shown in Fig. 5, we assume that the LDEF has cylindrical geometry and that the test specimen is a small, essentially planar article on the side surface. This being the case, it is possible to specify the normal to the test patch by a single vector, denoted $\hat{o}$, normal to the vertical (the yaw axis). Its azimuthal location about the $\hat{o}_3$ axis is specified by the angle λ:

$$\hat{o} = \hat{o}_1 \sin\lambda + \hat{o}_2 \cos\lambda \tag{8}$$

Since the test patch must remain at a fixed position on the spacecraft, the angle λ is constant.

Time Dependence of Geometrical Factors

We now briefly discuss the time dependence of the geometrical factors introduced earlier. Seven angles have been introduced: η_e, Ω_e, i_e, Ω, i, η, λ. The time dependence of $\eta_e(t)$ (the true anomaly associated with Earth's orbit about the Sun) is well known from Keplerian orbit theory. One can introduce the small eccentricity of Earth's orbit around the Sun ($e_e = 0.0167\ldots$) and solve Kepler's equation. However, numerical calculations[2] have shown that the effect of Earth's orbital ellipticity on LDEF temperatures is negligible; hence we take $e_e = 0$ here, whereupon

$$\eta_e(t) = 1.99 \times 10^{-7} t \tag{9}$$

Note that when $t = 3.156 \times 10^7$ s (i.e., after 1 yr), $\eta_e = 6.283$ (i.e., 2π).

Turning to the time dependence of Ω_e and i_e, we can assume that the north pole is inertially fixed (although, in reality, there is a slight periodic nutation of i_e with a period of 18.6 yr, and a secular precession of Ω_e with a cycle of 26,000 yr). We shall take $\Omega_e = 0$ and $i_e = 23.5$ deg.

As for Ω and i, at the low altitudes of interest here, we can assume that the LDEF orbit normal precesses about Earth's north pole according to the formula

$$\dot{\Omega} = -\frac{3\pi}{P} J_2 \left(\frac{r_e}{r_e + h}\right)^2 \cos i \tag{10}$$

where $r_e = 6.378 \times 10^6$ m, $J_2 = 1.083 \times 10^{-3}$, and P is the LDEF's orbital period in seconds. Note also, however, that the orbital period itself is slightly time dependent, owing to orbit contraction from atmospheric drag. That is, $h = h(t)$ in Eq. (10) and, moreover,

$$P(t) = 2\pi \left\{ \frac{[r_e + h(t)]^3}{\mu_e} \right\}^{1/2} \tag{11}$$

We shall also assume that there is no nutation of the LDEF orbit normal, and take $i = 24$ deg.

The true anomaly of the LDEF in its orbit about Earth is the most rapidly changing angle. Assuming a circular orbit, we have

$$\eta = \eta_0 + \frac{2\pi}{P} t \tag{12}$$

where η_0 is a reference value and the orbital period P was given, just before, by Eq. (11). The last of the seven angles, namely λ, refers to the location of a particular experimental test patch on the LDEF surface. Thus λ is constant. We shall take $\lambda = 10$ deg as a nominal value.

Shadowing

If the LDEF is in Earth's shadow (i.e., in eclipse), no solar radiation falls on any part of the spacecraft, including the test patch. Moreover, even if the LDEF is in sunlight, the patch may or may not see the Sun, depending on self-shadowing. We now consider the time-dependent geometrical conditions for Earth shadowing and self-shadowing.

Earth Shadowing (Eclipse)

Since the LDEF is in a low-altitude orbit, it is reasonable to neglect the orbital altitude in comparison with Earth's radius (and to neglect penumbral effects) and to say that the LDEF is in sunlight whenever the satellite's "up" direction $\hat{o}_3$ has a component toward the Sun; otherwise the LDEF is in Earth's shadow (i.e., in eclipse). This leads to the conclusion that the LDEF is in sunlight whenever $\hat{s} \cdot \hat{o}_3 \le 0$ and that it is in eclipse whenever $\hat{s} \cdot \hat{o}_3 > 0$. In fact, it will be convenient to define the vehicle Earth-shadowing function as follows:

$$\varphi_v(\eta_e, \Omega_e, i_e, \Omega, i, \eta) \triangleq \begin{cases} 1, & \text{when } \hat{s} \cdot \hat{o}_3 \le 0 \\ 0, & \text{when } \hat{s} \cdot \hat{o}_3 > 0 \end{cases} \tag{13}$$

Thus, when $\varphi_v = 1$, the vehicle is in sunlight; when $\varphi_v = 0$, the vehicle is in shadow.

To calculate $\hat{s} \cdot \hat{o}_3$, we note Eq. (1) for $\hat{s}$. Then

$$\hat{s} \cdot \hat{o}_3 = \begin{bmatrix} \cos \eta_e \\ \sin \eta_e \\ 0 \end{bmatrix}^T \boldsymbol{C}_{ab} \boldsymbol{C}_{be} \boldsymbol{C}_{ep} \boldsymbol{C}_{po} \begin{bmatrix} 0 \\ 0 \\ 1 \end{bmatrix} \tag{14}$$

The needed rotation matrices $\boldsymbol{C}_{ab}$, $\boldsymbol{C}_{be}$, $\boldsymbol{C}_{ep}$, and $\boldsymbol{C}_{po}$ have all been discussed earlier. (Some transposing may be necessary.) It can be shown from Eq. (14) that

$$\begin{aligned} \hat{s} \cdot \hat{o}_3 = {} & (\cos \Omega \cos \eta - \sin \Omega \cos i \sin \eta) \cos(\eta_e - \Omega_e) \\ & + [(\sin \Omega \cos \eta + \cos \Omega \cos i \sin \eta) \cos i_e \\ & - \sin i \sin \eta \sin i_e] \sin(\eta_e - \Omega_e) \end{aligned} \tag{15}$$

The time dependences of the angles η_e, Ω_e, i_e, Ω, i, and η have been given earlier.

Self-Shadowing

Even if the vehicle is in sunlight, the test patch will not see the Sun if there is self-shadowing, in which the test patch is shadowed by the rest of the vehicle. Since $\hat{o}$ has been defined as the unit outward normal to the test patch (see Fig. 5), the condition that sunlight fall on the test patch is that the LDEF not be in eclipse and that $\hat{s} \cdot \hat{o}_3 \le 0$. Thus, it is also convenient to define the function as follows:

$$\varphi(\eta_e, \Omega_e, i_e, \Omega, i, \eta, \lambda) \triangleq \begin{cases} -(\hat{s} \cdot \hat{o})\varphi_v, & \text{when } \hat{s} \cdot \hat{o} \le 0 \\ 0, & \text{when } \hat{s} \cdot \hat{o} > 0 \end{cases} \tag{16}$$

Thus, when $\varphi > 0$, the test patch (and therefore also the vehicle) can see the Sun; in fact, when $\varphi = 1$, the test patch sees the Sun flat on. When $\varphi = 0$, the test patch cannot see the Sun.

To calculate $\hat{s} \cdot \hat{o}$, we again note Eq. (1) for $\hat{s}$, and we note Eq. (8) for $\hat{o}$. Therefore,

$$\hat{s} \cdot \hat{o} = \begin{bmatrix} \cos \eta_e \\ \sin \eta_e \\ 0 \end{bmatrix}^T \boldsymbol{C}_{ab} \boldsymbol{C}_{be} \boldsymbol{C}_{ep} \boldsymbol{C}_{po} \begin{bmatrix} \sin \lambda \\ \cos \lambda \\ 0 \end{bmatrix} \tag{17}$$

The needed rotation matrices $\boldsymbol{C}_{ab}$, $\boldsymbol{C}_{be}$, $\boldsymbol{C}_{ep}$, and $\boldsymbol{C}_{po}$ have all been discussed earlier. An explicit form for the inner product in Eq. (17) is the following:

$$\begin{aligned} \hat{s} \cdot \hat{o} = {} & (-\cos \Omega \sin \eta \sin \lambda - \sin \Omega \cos i \cos \eta \sin \lambda + \sin \Omega \sin i \cos \lambda) \cos(\eta_e - \Omega_e) \\ & + \begin{bmatrix} -\cos i_e \sin \Omega \sin \eta \sin \lambda \\ + (\cos i_e \cos \Omega \cos i - \sin i_e \sin i) \cos \eta \sin \lambda \sin(\eta_e - \Omega_e) \\ - (\cos i_e \cos \Omega \sin i + \sin i_e \cos i) \cos \lambda \end{bmatrix} \end{aligned} \tag{18}$$

The time dependences of the angles η_e, Ω_e, i_e, Ω, i, η, and λ have been given earlier.

Normalized Solar Heat Flux

In this section we shall present computer plots of the normalized solar flux φ vs time. The detailed time dependence is quite complex, owing to the three simultaneously active time scales identified in the Introduction. In fact, we shall demonstrate that the fast-time-scale component of the flight data is associated primarily with the orbital motion of the LDEF around Earth. (Detailed comparisons between these computations and flight data are made difficult by the sampling rate used.) The slow-time-scale component of the flight data (the relatively slow oscillations of the order of 45 days) will be shown to be associated primarily with the precessional motion of LDEF's orbital plane. The very-slow-time-scale component (oscillations of the order of 300 days) is associated primarily with the annual motion of Earth around the Sun.

Orbital Motion Only

To build our understanding of the three-time-scale flux history in a logical sequence of steps, we begin by eliminating all but the orbital motion of the LDEF around Earth. That is, we temporarily eliminate orbital precession ($\dot{\Omega} \equiv 0$). We also stop Earth's motion around the Sun ($\dot{\eta}_e \equiv 0$)—something more easily done on a computer than in reality!

The flux history calculated for a one-day period is shown in Fig. 6. For about half the time, the LDEF is in eclipse; hence $\varphi_v = 0$ and consequently $\varphi = 0$. During the other half of the time, the patch spends 50% of the time in self-shadow, and consequently $\varphi = 0$. For the remaining time, φ is a piece of a sinusoid whose amplitude can be found from Eqs. (15), (16), and (18). If this plot were made[2] for an entire year (i.e., over 5600 orbits), it would be so compressed that it would appear to

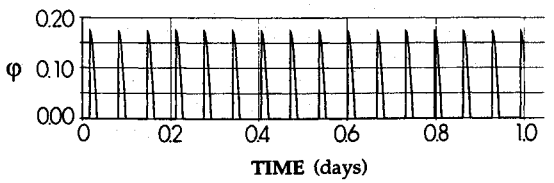

Fig. 6 Normalized solar flux, over a one-day period, with no LDEF orbital precession and with no rotation of Earth around the Sun.

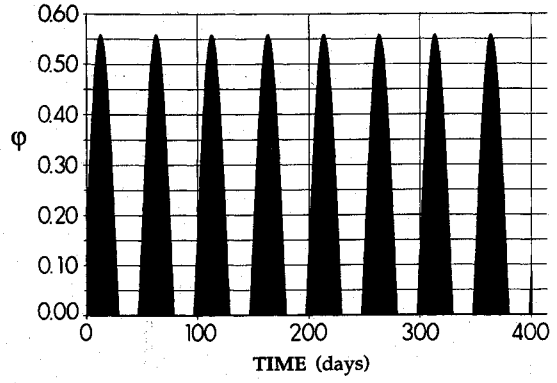

Fig. 7 Normalized solar flux, over 1 yr, with LDEF orbital precession, but with no rotation of Earth around the Sun.

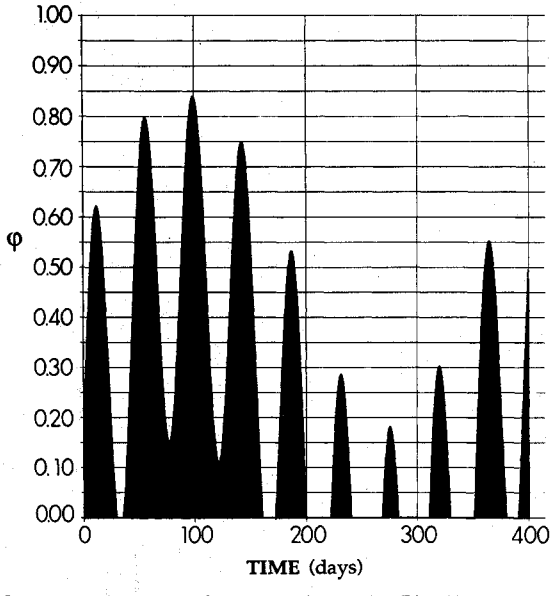

Fig. 8 Normalized solar flux, over 1 yr, with LDEF orbital precession, and with Earth's rotation around the Sun.

be a solid black rectangle. The variations within each orbit are lost when the horizontal scale is compacted by a factor of $10^{3.7}$.

Under current assumptions, $\hat{s}\cdot\hat{o}_3 = \cos\eta$, and $\hat{s}\cdot\hat{o} = -\sin\eta\sin\lambda$. Thus, from Eqs. (13) and (16), $\varphi = \sin\eta\sin 10$ if $\pi/2 \le \eta \le \pi$, and zero otherwise. This indicates that the maximum flux should be bounded by $\sin\lambda = \sin 10 = 0.174\ldots$, as shown in Fig. 6.

Orbital Motion, Plus Precession

To continue building our understanding of the three-time-scale flux history, we now add the second time scale: the orbital precession ($\dot{\Omega} \neq 0$). We continue, however, to suppress Earth's rotation around the Sun ($\dot{\eta} \equiv 0$). The calculated flux history is shown in Fig. 7. This plot looks "black" because the details within the 5600 orbits have been compressed, and details within each orbit are not visible. But it is clear that orbital precession causes a slow variation (about every 50 days) in the amplitude of φ.

From Eq. (18), under current assumptions,

$$\widehat{\hat{s}\cdot\hat{o}} = \left| (\sin\Omega\sin i)\cos\lambda \pm \sqrt{\cos^2\Omega + \cos^2 i\sin^2\Omega}\sin\lambda \right| \quad (19)$$

where the wide caret indicates the maximum amplitude achievable in any one orbit. Taking further the maximum amplitude achievable throughout a precessional cycle, we have

$$\widehat{\widehat{\hat{s}\cdot\hat{o}}} = |\sin i\cos\lambda + \cos i\sin\lambda| \equiv |\sin(i+\lambda)| \quad (20)$$

(The maximum can be shown to occur when $\Omega = \pi/2$.) Since we are currently assuming $i = 24$ deg and $\lambda = 10$ deg, this implies that $\sin(i+\lambda) = \sin 34 = 0.559\ldots$, as shown in Fig. 7.

Orbital Motion, Plus Precession, Plus Annual Variation

Finally, in our process of building understanding of the solar flux history, we come to the completion of the three time scales by adding the annual geometrical variation associated with Earth's orbit around the Sun. Figure 8 shows the calculated solar flux history for 1 yr. The chief features of the flight data (cf. Figs. 1 and 2) have thus been explained. Similar remarks apply to a comparison between Fig. 8 and plots like "Daily Time Averaged Orbital Heat Flux, Row 12, April 7,

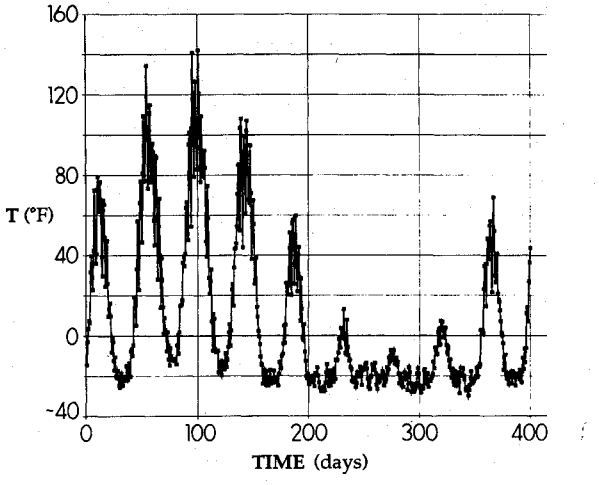

Fig. 9 Temperature history for 1 yr for a typical test patch (compare with flight data of Fig. 1).

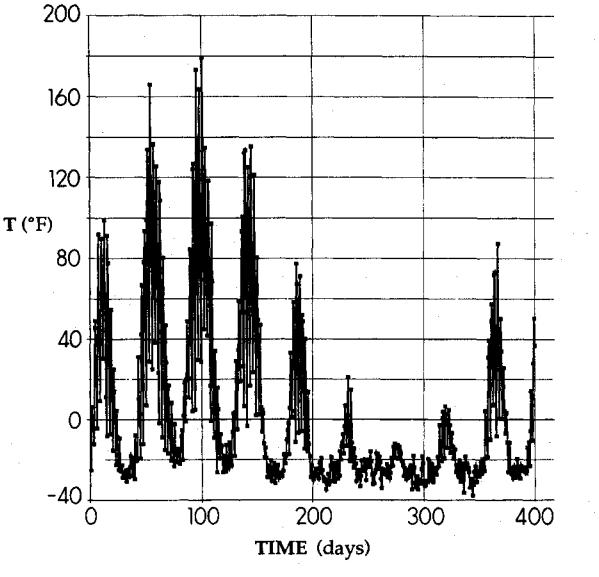

Fig. 10 Temperature history for a test patch with different thermal properties (compare with flight data of Fig. 2).

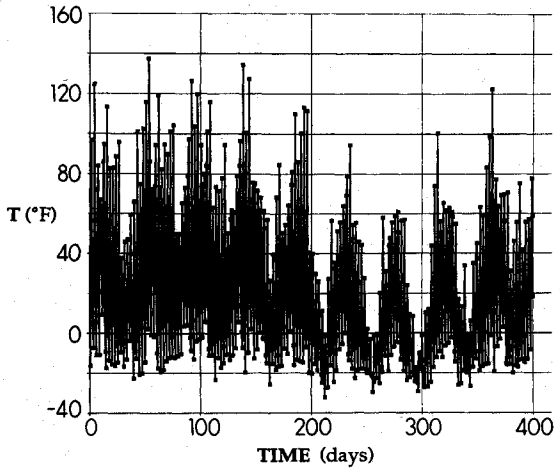

Fig. 11 Temperature history for a test patch at a different location on LDEF ($\lambda = 60$ deg).

1984—May 13, 1985," in Ref. 4. (Row 12 corresponds to $\lambda = 10$ deg.)

It must be borne in mind that LDEF temperature data is taken every 16 h. With respect to very-slow-time-scale (annual) variations, this represents very frequent sampling (i.e., ~550 samples/year). With respect to slow-time-scale (precessional) variations, this sampling rate is still quite frequent (i.e., ~68 samples/precessional period). However, with respect to the fast-time-scale (orbital) variations, the sampling rate is very infrequent (i.e., ~1 sample every 10 orbits!); not surprisingly, such a sampling rate can hardly be expected to pick out the details of intra-orbital variations.

Temperature Histories

Temperature histories similar to those in Figs. 1 and 2 can now be demonstrated; by so doing, we shall have attained a physical understanding of these histories. The average vehicle temperature T_v is of interest (see Appendix) but has been studied elsewhere.[2] Therefore, in the limited space available, we focus on the test patch temperature T.

Figure 9 shows T plotted over a period of about 1 yr for the parameters $\kappa = 10$, $\tau = 100$ h. The 16-h-sampled version is shown; for an unsampled (continuous-time) version, see Ref. 2. This plot is evidently similar qualitatively, and even semiquantitatively, to the flight data of Fig. 1. Figure 10 shows T (sampled) for $\kappa = 5.5$, $\tau = 20$ h (best-fit values); this should be compared with the flight data of Fig. 2. Finally, to illustrate the effect of the test patch being at a different location on the periphery of the vehicle (as represented by λ), Fig. 11 shows T, sampled and with the same thermal parameters as Fig. 10, when $\lambda = 60$ deg (instead of 10 deg). The temperature extremes are evidently more moderate at this point on the spacecraft.

Concluding Remarks

The physical origins of the features of LDEF surface temperature histories have been identified, as demonstrated from the comparison between calculations and flight data. Fast-time-scale variations are due to the orbital motion of the LDEF about Earth. These orbital effects, however, are not *directly* detectable from data samples every 16 h (i.e., roughly once every 10 orbits); the sampling process effectively filters out fast-time-scale (orbital) temperature variations.

Slow-time-scale variations are due to the precession of the LDEF's orbit about Earth's polar axis. This behavior, quite visible in the flight data, is explained herein as being due to orbital precession. Finally, the very-slow-time-scale behavior visible in the flight data has been shown to be due to the annual motion of Earth about the Sun.

Although detailed plots will not be presented here, it has also been determined by more extensive numerical study[2] of this model that the eccentricity of Earth's orbit about the Sun and the slow decrease in LDEF's orbital altitude (orbital decay) do not have important influences on LDEF temperatures.

Appendix: Simple Thermal Model

A simple phenomenological thermal model has been described in detail in Ref. 2. Here, we merely summarize the key equations from that model. Heat flow to the test patch is assumed to be from two sources only: the rest of the vehicle and directly from the Sun.

If T and T_v denote, respectively, the temperature of the test patch and the average temperature over the vehicle, the simple model assumes that

$$\tau \dot{T}(t) + T(t) = \kappa Q(t)$$

$$\tau_v \dot{T}_v(t) + T_v(t) = \kappa_v Q_{\odot v}(t)$$

where τ and τ_v are characteristic thermal time lags, κ and κ_v are heat input constants, and Q and $Q_{\odot v}$ are the total heat flux (heat per unit area per unit time) to the patch and to the vehicle. (The $\odot$ subscript is the standard symbol for the Sun.)

Furthermore, we set

$$Q(t) = Q_{\odot}(t) + Q_v(t)$$

$$Q_{\odot}(t) = \varphi(\eta_e, \Omega_e, i_e, \Omega, i, \eta, \lambda) Q_{\odot 0}$$

$$Q_{\odot v}(t) = \varphi_v(\eta_e, \Omega_e, i_e, \Omega, i, \eta) Q_{\odot v 0}$$

$$Q_v(t) = k_v \left[T_v(t) - T(t) \right]$$

$$Q_{\odot v 0} = \rho Q_{\odot 0}$$

where φ_v and φ are shadowing functions given earlier by Eqs. (13) and (16), k_v is a heat transfer constant for the patch with respect to the rest of the vehicle, ρ is a constant lying in the range $0 < \rho < 1$, and $Q_{\odot 0}$ (1404 $J \cdot m^{-2} \cdot s^{-1}$) is the heat flux from the Sun in the vicinity of the Earth. We shall use the values $k_v = 7$, $\rho = 0.352$, $\tau_v = 20$ h, and $\kappa_v = 1.0$. The test patch parameters τ and κ are assigned according to specific surface properties (i.e., are permitted to vary from patch to patch).

Acknowledgment

This work was supported by the Natural Sciences and Engineering Research Council of Canada (NSERC).

References

[1]Tennyson, R. C., Hansen, J. S., Mabson, G. E., Morison, W. D., and Kleiman, J., "Composite Materials in Space—Results from the LDEF Satellite," *Proceedings of the Sixth CASI Astronautics Conference,* Canadian Aeronautics and Space Institute, Ottawa, Canada, Nov. 1990.

[2]Berrios, W. M., "Long Duration Exposure Facility Post-Flight Thermal Analysis: Orbital/Thermal Environment Data Package," NASA Langley Research Center Rept. (unnumbered), June 1990.

[3]Hughes, P. C., "LDEF Temperature Histories: A Simple Theory," Univ. of Toronto Inst. for Aerospace Studies, Toronto, Canada, Rept. 340, Oct. 1990.

[4]Hughes, P. C., *Spacecraft Attitude Dynamics,* Wiley, New York, 1986, Chap. 2.

Antoni K. Jakubowski
Associate Editor